

Modelling and Controlling of an Offshore Container Structure

Mangapatnam Nymisha
Mechatronics
VIT University,
Vellore, Tamilnadu

Abstract—In this paper, a sliding-mode control for an offshore container crane is discussed. The offshore container crane is used to load/unload containers between a huge container ship (called the “mother ship”) and a smaller ship (called the “mobile harbor”), on which the crane is installed. The purpose of the mobile harbor is to load/unload containers in the open sea and transport them to shallower water where they can be offloaded at existing conventional ports, thereby obviating the need for expensive and expensive new facilities. The load/unload control objective is to suppress the pendulum motion (i.e., “sway”) of the load in the presence of the wave- and wind-induced movements (heave, roll, and pitch) of the mobile harbor. A new mechanism for lateral sway control, therefore, is proposed as well. A sliding surface is designed in such a way that the longitudinal sway of the load is incorporated with the trolley dynamics. The asymptotic stability of the closed-loop system is guaranteed by a control law derived for the purpose. The proposed new mechanism can suppress lateral sway, which functionality is not possible with conventional cranes. Simulation results are provided.

Keywords—Antisway control, mobile harbor, offshore container crane, ship motions, sliding-mode control.

1. INTRODUCTION

The rapid growth of the world economy has resulted in a high demand for freight transportation by large container ships. However, the current capacity of harbours is limited and due to the shallow waters and narrow areas, large container ships cannot dock at these ports. The solution to expand the capacity of the ports is unfeasible due to lack of investment funds and the negative impact on environmental sustainability. With this regard, a MHC concept was proposed to maximise the utilisation of container ships [1]. This solution allows a container ship anchoring in deep water to load and unload containers, then to transport them to their destination irrespective of the depth or narrow areas of any ports. The MHC system is an overhead crane system which is mounted on a mobile harbour to load and unload containers from the container ship to vessels and vice versa. Due to the harsh working environment, the MHC experiences more problems than conventional cranes that are fixed into the ground. One of the serious problems is the swing of the load caused by improper control of the trolley and influence of external disturbances such as the wave and wind. This is a serious problem, because it could cause extensive damage to surrounding devices and systems. Furthermore, if the swing of the container extends up to the end of the transfer, it becomes quite difficult to control the desired position of the

container [2]. In order to increase the productivity of the MHC system, all the crane motions should execute at high speed, and the load must be controlled to the desired position accurately. However, it is difficult to satisfy these requirements, because when the trolley is accelerated or decelerated, the suspended load will be swung undesirably. Moreover, the external disturbances caused by the wind and wave, and the continuously moving base make the trajectory of the load unpredictable. Therefore, controlling the load to a desired position is a challenge to solve. In general, two mechanical and electrical solutions have been proposed to anti-sway the load. The mechanical solution was applied successfully to suppress the longitudinal sway of the load in many tested cases. However, this method generated vibration, slow response time and high maintenance cost [3]. In most cases, the

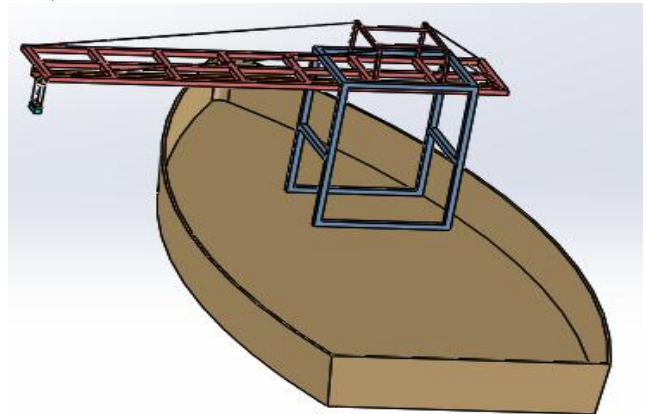


Fig. 1. The mobile harbour crane system.

electrical solution is popularly used to anti-swing the load. This solution was further classified into two kinds of control approach, open-loop control and closed-loop control. The open-loop control scheme proposed in [4] was not equipped with sensors. Its control objectives were based on predetermined speed control and trajectory, which have been simulated to dispose of the swing. This method is economical and stable with cranes that have a low natural frequency. However, it is inefficient with unstable plants, which are affected by disturbances. Meanwhile, the closed-loop control schemes were proposed as an anti-swing for the cranes. These schemes are equipped with many types of sensors to detect the sway angle of the load in linear/nonlinear controls [5-11]. The swing angle signal is processed by observation and estimation models before being transmitted to the controller. Several equipments were proposed to measure the swing

angle of the load. Yoshida et al. [10] proposed to use cameras as a non-contact sensor for visual feedback control of the crane. In this case, a 3D camera was installed on the trolley to measure the 3D position of the load. This approach is effective for cranes that experience disturbances. However, this vision system is cost consuming and difficult to maintain. In addition, longevity of vision devices is gradually reduced when they are exposed to the sea environment. In order to replace the vision system, Kim et al. [11] introduced a new vision sensor-less anti sway control system for container cranes, which uses an inclinometer that is placed on the spreader to detect the sway angle of the load. However, the common inclinometers lack high precision and have slow response times. Therefore, an expensive inclinometer is needed to achieve high precision. To achieve more economical, precise and quick responses, Park et al. [12] introduced a new approach, in which a tri-axial accelerometer was used to estimate the swing. In this approach, the swing angle is measured by the accelerometer based on the difference of the fixed points between the trolley and the spreader. Collaboratively, the above approaches were aimed to detect the swing angle effectively and to design a closed-loop control system to achieve an anti-swing of the load. These approaches have achieved the desired control objectives. However, the launch and deployment of a new control product into a real work environment require further time and cost for building, testing and verifying on the physical model. Hence, this paper proposes a virtual prototyping simulation technology that integrates ADAMS and MATLAB/Simulink. The ADAMS software is used to create the virtual mechanical model, with the possibility of virtual measurement of any parameters of any components in the virtual model. MATLAB software is well-known for designing a control system. Our co-simulation model of both software has a merit in simulating real behaviour of the mechanical system, and implementing the closed-loop control of the whole virtual prototype model. The simulations of results not only help designers to modify mechanical design but also improve the control method.

2. THE MHC SYSTEM MODELING

2.1. Necessity of developing a virtual prototyping for the MHC system Since the complexity of products has been increasing, in order to increase competition in production, the requirement of the product development cycle times should be reduced. Therefore, building a hardware prototype for testing has taken a majority of the time to launch a new product. The simulation technique based on the virtual prototype is proposed as an approach that significantly reduces manufacturing cost and time compared to the traditional build-and-test approach. The virtual prototyping approach is an integrating software solution that consists of modeling a mechanical system, simulating, and visualizing its 3D motion behaviour under real work operating conditions, and refining & optimising the design through iterative design studies [17]. The advantages of this simulation technique consist of conceiving a detailed model that is used in a virtual experiment in a similar way with a real scenario. The possibility to perform virtual measurements of any parameters and in any components of the mechanical model

can also be carried out conveniently. Fig. 4 shows the creation of a virtual prototype for the testing of the MHC system. In the design process of a mechatronic system, the mechanical design and control design stages are done separately with different software tools however the concept is the same. After the design, each separate model should be tested and verified for fulfilling the desired objectives, and finally a co-test should be implemented on the physical prototype to verify the proposed approaches. During testing on the physical prototype, if a problem appears in the interaction operation between two systems, the designer must refine the mechanical design and/or the control design to achieve a perfect system. In this method, the physical testing process is more simplified. It saves time and cost and reduces the risk of device damage caused by the conflict between both systems.

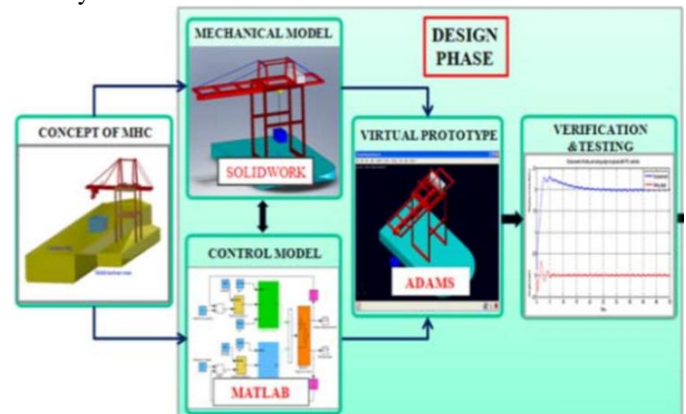


Fig. 2. The creation of the virtual prototype model for testing of the MHC system.

2.2. The virtual prototyping platform Fig. 5 shows a virtual prototyping platform which includes the following softwares: CAD-Computer Aided Design (SOLIDWORKS, CATIA, PROENGINEER); MBS-Multibody systems (ADAMS, SD-EXACT, PLEXUS); FEA- Finite Element Analysis (NASTRAN/ PATRAN, COSMOS, ANSYS) and Command & Control (MATLAB, EASY5, MATRIX) [17]. The CAD software is used to create the geometric model of the mechanical system. This model includes the rigid parts with shape and dimension of the physical prototype model, and it contains information about mass and inertia properties of these rigid parts. The CAD environment can perform simple motion testing with forces and torques. The geometry model is then exported from the CAD environment to the MBS environment using a file format as STEP (CATIA) or Parasolid.x_t (SOLIDWORKS). The MBS is the centre component of the virtual platform, and it is used for analysing, optimising, and simulating the kinematic and dynamic behaviour of the mechanical system under real operating conditions. The FEA software is used for modeling flexible components. The MBS has an ability to transfer loads to FEA and receive the flexible components feedback from FEA. This feature enables the capturing of inertia and compliance effects, and predicting loads with greater accuracy, hence obtaining more realistic results. Command & Control (C&C) is a software product which is used to design the control system. This software exchanges information with the MBS software. The exchange process creates a closed

loop in which the outputs from the MBS model are the inputs for the control system and vice-versa. The outputs from MBS

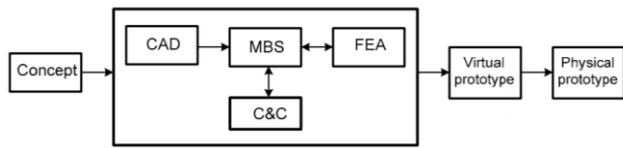


Fig. 3. The virtual prototyping platform.

model are measured parameters that are necessary for control, and the outputs from control system effect on the MBS simulation.

2.3. Modeling a MHC mechanical system In order to generate the mechanical model of the MHC system, all components or elements which have the shape and dimensions of the physical model are modeled as 3D solid by SOLIDWORKS. These elements were created with the geometric constraints showing the characteristics of the MHC system. This mechanical model tested and evaluated the “real” behaviour through applying the torque and force to drive the elements of the MHC model. It was then exported to ADAMS to execute the dynamic simulation. In the ADAMS/view environment, a MHC modeling is created. The modeling process is constructed as the following sequence for an easy modification in the design phase. Firstly, the geometrical parameters of the parts such as material, mass, and density must be defined, and then mass and inertial matrices are generated automatically. These parts are connected one with other, respectively to the floating coordinate, using the following geometric constraints. These constraints are described as follows. The center of floating mass coordinate (denoted by 1) is fixed on the centre of the Cartesian coordinate in ADAMS using a revolute joint. The floating motion is swayed based on the wave disturbance function. The frame (denoted by 2) is mounted on the floating and moved along the floating using a translational joint. The trolley (denoted by 3), which is driven by force that is generated from a motor, is slid on the frame along the x direction using the translational joint. The container (denoted by 4) is joined to the trolley using a spherical joint, and is moved following the trolley motion. Fig. 4 shows the virtual prototyping of the mechanical model of the MHC system. The simulation process on the virtual prototyping model is implemented to investigate the real behaviour of the mechanical MHC model. The parameter values used in the Adams simulation are presented in Table 1.

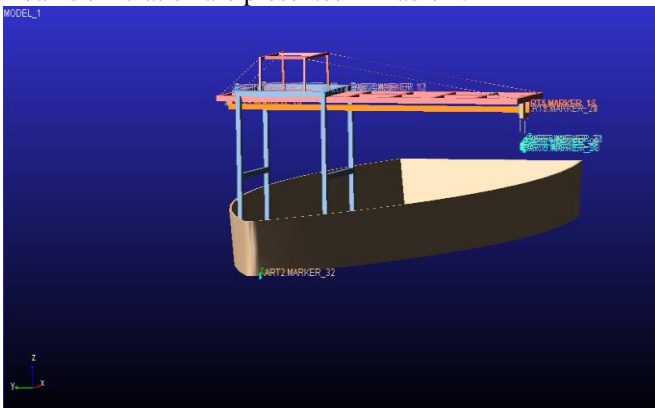


Fig. 4. The Adams model of the MHC system.

Table 1. The parameter values used in the simulation.

Parameters	Values
Simulation time	$t = 50 \text{ sec}$
The trolley trajectory:	
- Translation follows the x axis	$x = \text{step}(\text{time}, 0, 0, 30, 3.8)$
- Translation follows the y axis	$y = \text{step}(\text{time}, 30, 0, 50, 3)$
Crane height	$h = 3 \text{ m}$
Rope length	$l = 1.2 \text{ m}$
Trolley mass	$m = 127 \text{ kg}$
Container mass	$m = 148 \text{ kg}$
Wave disturbance function	$S_w(t) = 0.02\sin(1.5\text{time}) \text{ rad}$

3. DEVELOPING A CONTROL SYSTEM FOR THE MHC MECHANISM

3.1. Creating an adams_sys in MATLAB/Simulink Constructing a control system for the virtual MHC model is necessary for co-simulation of the two separate simulation programs into a whole system. The control design is developed based on ADAMS/Control and MATLAB/Simulink. To export the virtual MHC mechanical model from ADAMS to MATLAB environment,

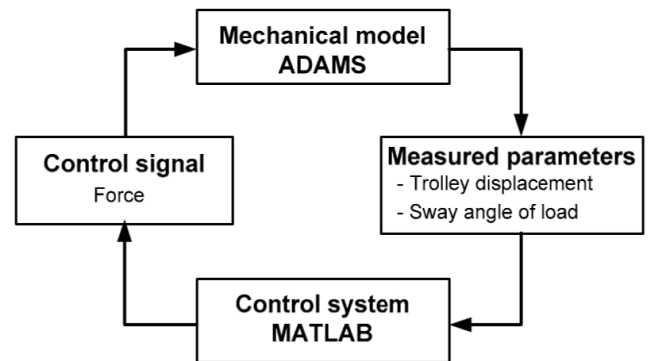


Fig. 5. The connection of Adams and Matlab in the co-simulation model.

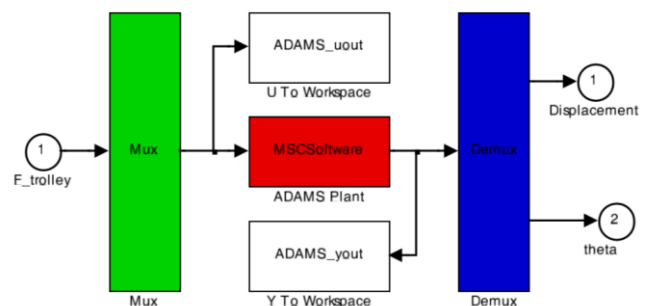


Fig. 6. The ADAMS block in adams_sys.

the input and output variables are firstly defined in the ADAMS model. The input signal is the force that controls the trolley movement. Meanwhile, the output signals are the measured parameters of the trolley position and the swing angle of the load, respectively. Subsequently, this model is exported to MATLAB/ Simulink. Fig. 5 shows the connection between Adams and Matlab in the co-simulation model. In MATLAB environment, a .m file and an adams_sys are created. The adams_sys presents the non-linear MSC.ADAMS model (i.e., the MHC mechanical system) as shown in Fig. 6. The ADAMS block is created based on the information from the .m file [17]. This adams_sys is used to build a control system in

MATLAB/Simulink in which the input signal is the generated signal from the controller, and the output signals are the measured values of the trolley displacement and swing angle of the load, respectively.

4.2. Controller design As analysed above, the MHC model is a nonlinear system that is operated in harsh environments with external disturbance and system parameter variations. In this condition, a traditional PID controller, with three PID gains (proportional gain K_P , integral gain K_I , and derivative gain K_D) are fixed, cannot be applied for controlling the position and angle of the MHC system. In order to achieve system robustness against parameter variations, this paper proposes an adaptive sliding mode PID controller (ASMP), which combines the advantages of PID and sliding mode controllers [18]. Fig. 11 shows the block diagram of the adaptive sliding mode PID control system for the MHC.

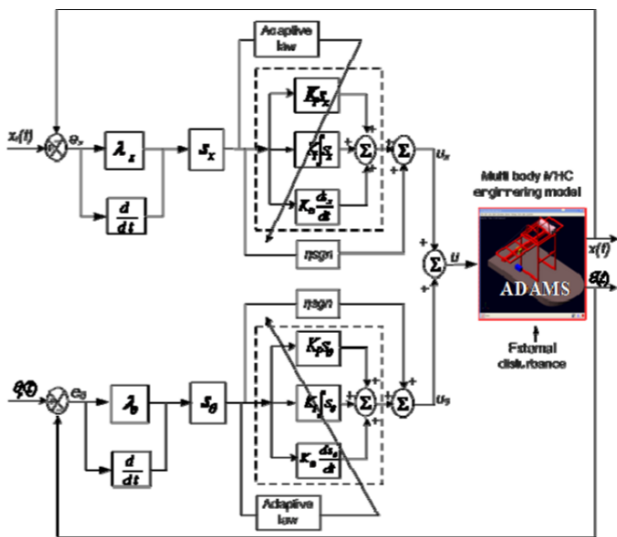


Fig. 7. Block diagram of adaptive sliding mode PID control system for the MHC.

Several previous researchers applied the sliding mode controller method for the uncertainty system [9,16,24]. Sliding mode control (SMC) is a modern control method that uses state-space approach to analyse such a system. The advantage of SMC is its robustness against system parameter variations and external disturbances. The way SMC deal with uncertainty is to drive the plants state trajectory onto a sliding surface and maintain the error trajectory on this surface for all subsequent times. The sliding surface is defined such that the state tracking error converges to zero with input reference [24]. An additional adaptive law is developed in such a way that the PID control gains can be updated online with an adequate adaptation mechanism that is adaptive with the variations of system parameters and external disturbances. Based on the nonlinear systems that were defined in Wang's study [16], this paper considers the MHC system as a nonlinear system with a single-input and multi-output, and the assumption that the trolley motion along the X-direction, the couple systems can be expressed in the following form:

$$\begin{aligned} \dot{x}_1 &= x_2, \\ \dot{x}_2 &= f_1(X) + b_1(X)u_x + d_1(t), \\ \dot{x}_3 &= x_4, \\ \dot{x}_4 &= f_2(X) + b_2(X)u_\theta + d_2(t), \end{aligned} \tag{5}$$

where $X = (x_1, x_2, x_3, x_4)$ is state variables vector that represents the position and velocity of trolley, the sway angle and angle velocity of payload. The $f_1(X)$, $f_2(x)$, $b_1(X)$ and $b_2(X)$ are the nonlinear functions. The $d_1(t)$ and $d_2(t)$ are the bounded lumped disturbances which include the system parameter variations and external disturbances (i.e., they satisfy $|d_1(t)| \leq d_{1M}$ and $|d_2(t)| \leq d_{2M}$, where d_{1M} , d_{2M} are known non negative constants), and u is the control input to control the crane trolley position and sway angle of payload to achieve the desired objectives.

From (5), the MHC system has two subsystems: the positioning subsystem of the crane trolley, and the anti-swing of payload. The sliding surfaces of the two subsystems are defined as:

$$\begin{aligned} s_x &= \dot{e}_x + \lambda_x e_x, \\ s_\theta &= \dot{e}_\theta + \lambda_\theta e_\theta. \end{aligned} \tag{6}$$

In this work, a control input u was designed to control the trolley position and suppress the swing angle of the load simultaneously. The design methods for these two controllers are similar, hence the method for designing the trolley position controller is presented. The sliding surface of the trolley position controller is rewritten as.

$$s_x = \dot{e}_x + \lambda_x e_x, \tag{7}$$

where $e_x = x_d - x$, x_d is the desired position; x is the measured position; and λ_x is a positive constant.

Derivating (7)

$$\dot{s}_x = \ddot{e}_x + \lambda_x \dot{e}_x = \ddot{x}_d - \ddot{x} + \lambda_x \dot{e}_x. \tag{8}$$

Substituting $\dot{x}_2 = \dot{x}$ from (5) into (8), we have

$$\dot{s}_x = \ddot{x}_d - f_1(X) - b_1(X)u_x - d_1(t) + \lambda_x \dot{e}_x. \tag{9}$$

The control input u of PID controller is designed based on (9)

$$u_{PID} = \frac{1}{b_1(X)} [\ddot{x}_d - f_1(X) - d_1(t) + \lambda_x \dot{e}_x] = AB + \varepsilon, \quad (10)$$

where $A = [K_P \ K_I \ K_D]$: vector of the gain of PID controller; $B = \left[s_x \int s_x \frac{ds_x}{dt} \right]^T$: basic vector of PID controller; ε is an approximate error.

The control signal u_x of the position controller is determined as:

where \hat{A} is estimated value of vector A , $\hat{A} = [\hat{K}_P \ \hat{K}_I \ \hat{K}_D]$; u_h is control signal of the auxiliary controller.

Substituting (11) into (9) yields:

$$\begin{aligned} \dot{s}_x &= \ddot{x}_d - f_1 - b_1 [\hat{A}B + u_h] + \lambda_x \dot{e}_x - d_1 \\ &= b_1 \tilde{A}B + b_1 \varepsilon - b_1 u_h, \end{aligned} \quad (12)$$

where $\tilde{A} = A - \hat{A}$ is estimation error.

In order to prove the stability, the Lyapunov function can be used.

$$V = \frac{1}{2} s_x^2 + \frac{1}{2\gamma} \tilde{A}^2 \quad (13)$$

Derivating (13) yields:

$$\begin{aligned} \dot{V} &= s_x \dot{s}_x + \frac{1}{\gamma} \tilde{A} \dot{\tilde{A}} \\ &= s_x (b_1 \tilde{A}B + b_1 \varepsilon - b_1 u_h) + \frac{1}{\gamma} \tilde{A} \dot{\tilde{A}} \\ &= \left(s_x b_1 B + \frac{1}{\gamma} \dot{\tilde{A}} \right) \tilde{A} + s_x b_1 \varepsilon - b_1 u_h s_x \\ &\leq 0. \end{aligned} \quad (14)$$

From (14), we have

$$\left(s_x b_1 B + \frac{1}{\gamma} \dot{\tilde{A}} \right) = 0. \quad (15)$$

Hence, $\dot{\tilde{A}} = -\dot{\hat{A}} = -\gamma s_x b_1 B$.

The three PID controller gains including K_P , K_I , and K_D are on-line updated by the following adaptive laws

$$\begin{aligned} \dot{\hat{K}}_P &= \gamma s_x b_1 s_x, \\ \dot{\hat{K}}_I &= \gamma s_x b_1 \int s_x, \\ \dot{\hat{K}}_D &= \gamma s_x b_1 \frac{ds_x}{dt}. \end{aligned} \quad (16)$$

Considering (14)

$$\begin{aligned} \dot{V} &= b_1 \varepsilon s_x - b_1 \eta \operatorname{sgn}(s_x) s_x \\ &= b_1 \varepsilon s_x - b_1 \eta |s_x| < b_1 |s_x| (|\varepsilon| - \eta) < 0 \end{aligned} \quad (17)$$

$$\Rightarrow \eta > |\varepsilon|,$$

where $u_h = \eta \operatorname{sgn}(s_x)$ is the sign function.

$$\operatorname{sgn}(s_x) = \begin{cases} 1 & \text{if } s_x > 0 \\ 0 & \text{if } s_x = 0 \\ -1 & \text{if } s_x < 0 \end{cases} \quad (18)$$

Equation (14) proves that the sliding surface is stability. The control input for controlling the MHC model is composed of the trolley position control input u_x and the angle control input u_θ as:

$$u = u_x + u_\theta. \quad (19)$$

5. SIMULATION RESULTS

In this section, the simulation is implemented in the MHC virtual model under the condition of wave disturbance and system parameter variations. The wave disturbances are changed by the height and frequency of the sea wave. Meanwhile, the system parameters (load and stretch of rope) are changed by the length and mass. The values of these simulation parameters are given in Table 2. According to Solihin et al. [19], the control goals of the ASMP controllers, including tracking the position of the trolley and suppressing the sway angle of the load, are considered in the following criteria. In order to carry out quick motions with small overshoot, the ASMP controller for the trolley position is optimised by considering the following desired specifications:

- Overshoot $\leq 2\%$

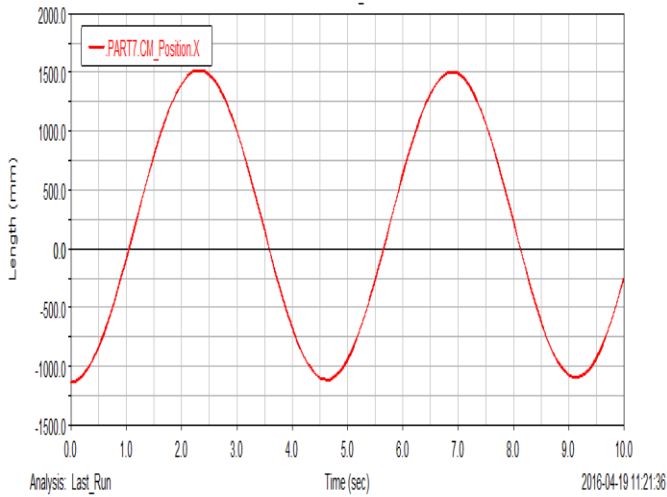
- Settling time ≤ 5 s
- Steady state error $\leq \pm 15\%$.

On the other hand, in order to suppress the swing angle quickly, the ASMP controller is optimised based on the following desired specifications:

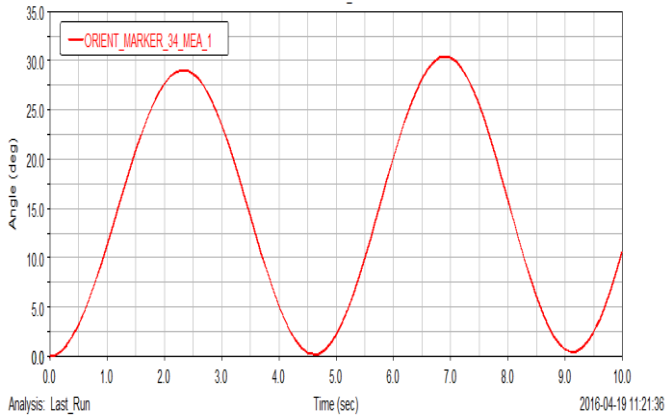
- Settling time ≤ 5 s
- Residual swing $\leq \pm 0.05$ rad.

Table 2. The system parameters for simulation.

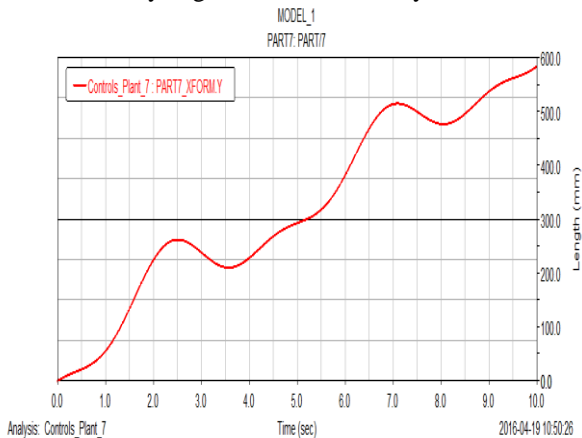
Parameters	Values
Simulation time (t)	30 sec
The control objectives:	
- Desired trolley position (X_d)	2.0 m
- Desired sway angle of load (θ_d)	0 rad
Model parameters:	
- Crane height (h)	3 m
- Rope length (l)	1.2 m; 1.5 m
- Trolley mass (m_t)	127 kg
- Load mass (m_l)	148 kg; 350kg
Disturbance parameters:	
- Sea wave height (h_w)	0.02 m; 0.04 m
- Sea wave frequency (f_w)	1.5 rad/sec; 3 rad/sec
Control gains of the ASMP:	
- Tracking the desired position	$\lambda = 200, \gamma = 1e-15,$
- Tracking the desired angle	$b = 1/127, \lambda = 200,$
	$\gamma = -1e-9, b = 1$



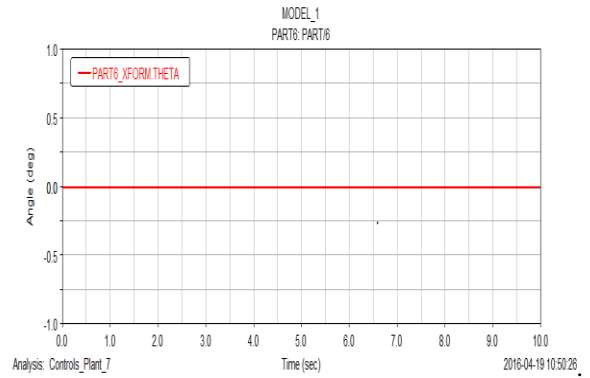
Trolley position without control system



Sway angle without control system



Trolley position with control system



Sway angle with control system

6. CONCLUSION

In this paper, the dynamic behaviour simulation of the MHC system using ADAMS was presented. The test was executed to verify the mechanical behaviour of the MHC system in the virtual model in accordance with the actual mechanical system. The co-simulation model of the MHC control system based on the ASMP control method was established in ADAMS and MATLAB/Simulink in order to study the performances of the ASMP controller in the cases of disturbance and system parameter variations. The simulation results show that the ASMP controllers are robust in regard to disturbance and system parameter variations. Fig. 20 shows the testbed of UOU, which was manufactured at University of Ulsan Korea. The verification of the proposed ASMP method will be carried out on this testbed and the results of the experiment study will be presented in a future paper. In this approach, the analysis and evaluation of the dynamic mechanical behaviour of the MHC system can be executed through co-simulation method that uses the commercial software to replace the traditional build-and-test approach. Significantly, this approach can support the designers to modify the mechanical and control designs to eliminate errors and increase the accuracy.

REFERENCES

- [1] K. Elissa, "Title of paper if known," unpublished.
- [2] R. Nicole, "Title of paper with only first word capitalized," J. Name Stand. Abbrev., in press.
- [3] Y. Yorozu, M. Hirano, K. Oka, and Y. Tagawa, "Electron spectroscopy studies on magneto-optical media and plastic substrate interface," IEEE Transl. J. Magn. Japan, vol. 2, pp. 740-741, August 1987 [Digests 9th Annual Conf. Magnetics Japan, p. 301, 1982].
- [4] M. Young, The Technical Writer's Handbook. Mill Valley, CA: University Science, 1989.
- [5] H. Park, D. Chwa, and K.-S. Hong, "A feedback linearization control of container cranes: varying rope length," International Journal of Control, Automation, and Systems, vol. 5, no. 4, pp. 379-387, 2007.
- [6] Q. H. Ngo and K. S. Hong, "Sliding mode antisway control of an offshore container crane," IEEE/ASME Trans. on Mechatronics, vol. 17, no. 2, pp. 201-209, April 2012.
- [7] Y. Yoshida and H. Tabata, "Visual feedback control of an overhead crane and its combination with time-optimal control," Proc. of IEEE/ASME International Conference Advanced Intelligent Mechatronics, pp. 1114-1119, July 2008.
- [8] Y. S. Kim, H. Yoshihara, N. Fujioka, H. Kasahara, H. Shim, and S. K. Sul, "A new vision-sensorless anti-sway control system for container cranes," Proc. of Industry Applications Conference of 38th IAS Annual Meeting, vol. 1, pp. 262-269, October 2003.

- [9] K. R. Park and D. S. Kwon, "Swing-free control of mobile harbour crane with accelerometer feed-back," Proc. of International Conference on Control, Automation and Systems, pp. 1322-1327, Oct. 2010.
- [10] Q. H. Ngo, K. S. Hong, K. H. Kim, Y. J. Shin, and S. H. Choi, "Skew control of a container crane," Proc. of International Conference on Control, Automation and Systems, pp. 1490-1494, Oct. 2008.
- [11] J. J. Jang and G. J. Shinn, "Analysis of maximum wind force for offshore structure design," Journal of Marine Science and Technology, vol. 7, no. 1, pp. 43-51, 1999.
- [12] P. T. D. Spanos, "Filter approaches to wave kinematics approximations," Journal of Applied Ocean Research, vol. 8, no. 1, pp. 2-7, Jan. 1986.
- [13] W. Wang, J. Yi, D. Zhao, and D. Liu, "Design of a stable sliding-mode controller for a class of second-order underactuated systems," IEE Proc.-Control Theory Appl., vol. 151, no. 6, pp. 683-690, Nov. 2004.
- [14] C. Alexandru and C. Pozna, "Dynamic modeling and control of the windshield wiper mechanisms," Journal WSEAS Transactions on Systems, vol. 8, no. 7, pp. 825-834, July 2009.
- [15] T. C. Kuo, Y. J. Huang, C. Y. Chen, and C. H. Chang, "Adaptive sliding mode control with PID tuning for uncertain systems," Engineering Letters, vol. 16, no. 3, pp. 311-315, 2008.
- [16] M. I. Solihin and Wahyudi, "Sensorless anti-swing control for automatic gantry crane system: model-based approach," International Journal of Applied Engineering Research, vol. 2, no. 1, pp. 147-161, 2007.
- [17] D. G. Ullman, The Mechanical Design Process